Proceedings of the 2005 IEEE
International Conference on Robotics and Automation
Barcelona, Spain, April 2005

Metric-Based Scan Matching Algorithms for Mobile Robot Displacement Estimation

Javier Minguez
I3A, Dpto. de Informática e Ing. de Sistemas
Universidad de Zaragoza, Spain
jminguez@unizar.es

Florent Lamiraux
LAAS-CNRS
Toulouse, France
florent@laas.fr

Luis Montesano
I3A, Dpto. de Informática e Ing. de Sistemas
Universidad de Zaragoza, Spain
montesano@unizar.es

***Abstract*— This paper presents a metric-based matching algorithm to estimate the robot planar displacement by matching dense two-dimensional range scans. The contribution is a geometric distance that takes into account the translation and orientation of the sensor at the same time. This result is used in the two steps of the matching - estimation process. The correspondences between scans are established with this measure and the minimization of the error is also carried out in terms of this distance. As a result, the translation and rotation are compensated in this framework simultaneously. In fact, this is the contribution with respect to previous work that addressed only translation or translation and rotation but separately. The new technique has been implemented and tested on a real vehicle. The experiments illustrate how it is more robust and accurate than prior techniques. At the end of the paper, we give an extension of our distance measure to 3D range-data matching problems.**

I. INTRODUCTION

One of the key issues in autonomous mobile robots is to keep track its position. Usually this problem is addressed by using the on board sensors to gather information of the environment for localization and mapping purposes. Many applications in robotics use techniques to estimate the robot displacement among successive range measurements. This paper presents a new method that achieves this goal. In robotics these techniques have been successfully applied to a wide range of issues as an ameliorated odometry. For example to improve the performance of simultaneous localization and mapping algorithms [21], [9], [11], to build local maps for indoor and outdoor navigation [15], [12], [16] and to implement people tracking systems for mobile platforms [20]. Furthermore, the pattern recognition and machine vision communities have also addressed the sensor matching problem in the context of 3D data registration, object recognition or scene understanding [19], [13]. In this paper, we also give the perspective to apply our technique to these communities.

The objective of the scan matching techniques is to compute the relative motion of a vehicle between two consecutive configurations by maximizing the overlap between the range measurements obtained at each configuration. They usually assume an initial estimation of the relative pose of the scans that is provided by the vehicle odometry.

One of the main differences between the existing algorithms is the usage or not of high-level entities such as lines or planes. In structured environments, one can assume the existence of polygonal structure in the environment [8], [6], [4]. These methods are fast and work quite well for indoor environments. However, they limit the scope of application to the extraction of geometric features that are not always available in unstructured environments. On the other hand, a great deal of work has been done to perform in any type of scenario dealing with raw data. Roughly, these techniques are based on an iterative process that estimates the sensor displacement that better explains the overlap between the scan measurements. For example [3] constructs a piecewise continuous differentiable density that models on a grid the probability to measure a point, and then, apply the Newton's algorithm. By converting the scans to statistical representations, [22] iteratively compute the crosscorrelation that results in the displacement. In [7] the motion parameters are estimated using a constrained velocity equation for the scanned points.

However, the most popular methods usually follow the Iterative Closest Point (ICP) algorithm (principle borrowed from the computer vision community [2]). They are based on an iterative process where they first compute the correspondences between the scans, and then they minimize the distance error to compute the sensor displacement [14], [18], [10], [1]. This process is repeated with this new estimate until convergence. A common feature of most versions of ICP is the usage of the Euclidean distance to establish the correspondences and to apply the least squares. However, this distance does not account for the fact that points far from the sensor could be far from its correspondent due to rotations of the sensor. To overcome this limitation [14] proposed to compute two set of correspondents, one by the Euclidean distance and other by the angular distance (to capture the sensor rotation). The gain in accuracy is however lost in complexity and convergence since the method builds two sets of matchings and performs two minimizations (rotation and translation) at each iteration. We understand that this is a central problem of the ICP algorithms: to find a way to measure (to find the *closest* correspondent and to apply the minimization) in such a way that it captures the sensor translation and rotation at the same time.

Our contribution resides in the definition of a new distance measure in the image space of the sensor that takes into account both, translation and rotation at the same time. The distance between two points is the norm (in a sense we are going to define) of the smallest rigid body

0-7803-8914-X/05/$20.00 ©2005 IEEE.

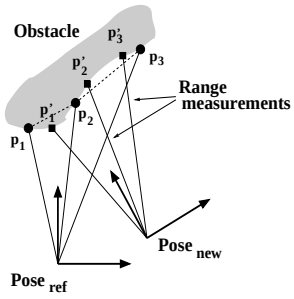

Fig. 1. This Figure depicts the scan-matching problem: to compute the sensor relative displacement between poses using the range information. Due to the discrete nature of the data it is assumed local structure in the reference scan (a segment that joins successive points).

transformation that leads a point to the other one. I.e our distance naturally depends on translation and rotation. We use this distance in both steps of the ICP algorithm:

1) matching of each point of a scan with the closest feature of the other scan in terms of our distance,
2) computation of relative displacement by least square minimization of the errors (in terms of our distance).

With this formulation we obtain results that ameliorate the algorithm that we were using [14] (the most used algorithm for scan matching) in terms of robustness, convergence and precision. Furthermore, we present in the paper the extension to the 3D problem, which could be used by the robotics, computer vision and graphics communities that use the ICP algorithm to address sensor motion estimation, location and map building, object recognition, pattern analysis, image registration, and scene understanding among others.

The paper is distributed as follows: in Section II we describe the ICP algorithm. In Section III-C we show how to use our distance to match points of two laser scans and we express the least square criterion we minimize, based on this distance measure. In Section IV, we discuss the experimental results and we compare our method with existing methods. Finally we draw our conclusions in Section V and we discuss possible extensions and future work in Section VI.

II. The Iterative Closest Point (ICP) algorithm

Given a reference scan S_{ref}, the new scan S_{new} and a rough estimation q_0 of the relative displacement of the sensor between the scans, the objective is to estimate the real displacement $q = (x, y, \theta)$ between them (Figure 1).

The ICP algorithm addresses this problem with an iterative process in two steps. At each iteration k, there is a search of correspondences between the points of both scans. Then the estimation of relative displacement q_k is improved through a minimization process. The process is repeated until convergence:

1) First let place each point p'_i of S_{new} in the system of reference S_{ref} using the estimation q_k, $p''_i = q_k(p'_i)$. Then, due to the discrete nature of the data, it is assumed a local structure in S_{ref} between successive points (p_i, p_{i+1}) of S_{ref} [14] (Figure 1). Thus, the correspondent point to p''_j is the closest point p_j belonging to one of the segments $[p_i\ p_{i+1}]$:
$$min\{d(p''_j, [p_i\ p_{i+1}])\} \quad (1)$$
The result is a set C of n correspondences (p_j, p''_j).
2) Compute the displacement estimation q_{min} that minimizes the mean square error between pairs of C. The criterion to minimize is q:
$$E_{dist}(q) = \sum_{i=1}^{n} d(p_j, q(p''_j))^2 \quad (2)$$
If there is convergence the estimation is q_{min}, otherwise we iterate again with $q_{k+1} = q_{min}$.

The ICP uses the Euclidean distance in both steps of the algorithm. The contribution of this work is a distance that takes into account translation and rotation simultaneously. In order to use this new concept in the ICP we need to define the distance, give the expression of distance point to segment, and formulate the least squares in terms of the new distance. In the next section we address these issues.

III. Distance Measure and Tools Associated

In this section, we introduce first our distance measure in the plane, defined as the minimum norm among the rigid body transformations that move a point to another one.

A. Distance point to point

A rigid body transformation in the plane is defined by a vector $q = (x, y, \theta)$ representing the position and orientation ($-\pi < \theta < \pi$) of the scanner sensor in the plane. We define the norm of q as :
$$\|q\| = \sqrt{x^2 + y^2 + L^2\theta^2} \quad (3)$$
where L is a positive real number homogeneous to a length. Given two points $p_1 = (p_{1x}, p_{1y})$ and $p_2 = (p_{2x}, p_{2y})$ in $\mathbf{R}^2$, we define a distance between p_1 and p_2 as follows:
$$d_p(p_1, p_2) = min\{\|q\| \text{ such that } q(p_1) = p_2\} \quad (4)$$
where
$$q(p_1) = \begin{pmatrix} x + \cos\theta\ p_{1x} - \sin\theta\ p_{1y} \\ y + \sin\theta\ p_{1x} + \cos\theta\ p_{1y} \end{pmatrix} \quad (5)$$
It can be easily checked that d_p is a real distance satisfying for any p_1 and p_2:

1) $d_p(p_1, p_2) = d_p(p_2, p_1)$
2) $d_p(p_1, p_2) = 0$ implies $p_1 = p_2$
3) $d_p(p_1, p_3) \leq d_p(p_1, p_2) + d_p(p_2, p_3)$

Unfortunately, there is no closed form expression of the above distance w.r.t. the coordinates of the points. However, we can compute an approximation valid when the minimum norm transformation is small, by linearizing (5) about $\theta = 0$. The set of rigid-body-transformations satisfying $q(p_1) = p_2$ can be approximated by the set of solutions (x, y, θ) of the following system:
$$x + p_{1x} - \theta\ p_{1y} = p_{2x}$$
$$y + \theta\ p_{1x} + p_{1y} = p_{2y}$$

The set of solutions is infinite and can be expressed by:

$$\begin{aligned} x &= p_{2x} - p_{1x} + \theta\ p_{1y} \\ y &= p_{2y} - p_{1y} - \theta\ p_{1x} \end{aligned}$$

where θ is a parameter for the set of solutions. Let us recall that according to (4), we need to find the solution that minimizes the norm of $q = (x, y, \theta)$. For a given θ, this norm is given by the following equation, after substituting the above expressions of x and y into (3):

$$\|q\| = (\delta_x + \theta\ p_{1y})^2 + (\delta_y - \theta\ p_{1x})^2 + L^2\theta^2$$

where $\delta_x = p_{2x} - p_{1x}$ and $\delta_y = p_{2y} - p_{1y}$. Expanding the above expression, we obtain a polynomial of degree 2 in θ:

$$\|q\|^2 = a\theta^2 + b\theta + c$$

with $a = p_{1y}^2 + p_{1x}^2 + L^2$, $b = 2(\delta_x p_{1y} - \delta_y p_{1x})$ and $c = \delta_x^2 + \delta_y^2$. Notice that $a > 0$ implies that this expression has a unique minimum for $\theta = -b/(2a)$ and the value of this minumum is given by

$$\begin{aligned} \|q\|^2 &= \frac{-b^2 + 4ac}{4a} \\ &= \frac{-(\delta_x p_{1y} - \delta_y p_{1x})^2 + (p_{1y}^2 + p_{1x}^2 + L^2)(\delta_x^2 + \delta_y^2)}{p_{1y}^2 + p_{1x}^2 + L^2} \\ &= \delta_x^2 + \delta_y^2 - \frac{(\delta_x p_{1y} - \delta_y p_{1x})^2}{p_{1y}^2 + p_{1x}^2 + L^2} \end{aligned}$$

Finally, the distance between p_1 and p_2 is approximated by:

$$d_p^{ap}(p_1, p_2) = \sqrt{\delta_x^2 + \delta_y^2 - \frac{(\delta_x p_{1y} - \delta_y p_{1x})^2}{p_{1y}^2 + p_{1x}^2 + L^2}} \quad (6)$$

Notice that as expected, our distance is smaller than the Euclidean distance, since this latter is the norm of the translation between p_1 and p_2 and therefore is bigger than the minimum norm.

To better understand the properties of this distance measure, let us compute the iso-distance curves. Again, we do not have the exact expression of the iso-distance curves but if we use approximation (6), we can prove that the iso-distance curves relative to d_p^{ap}:

$$\{p_2 \in \mathbf{R}^2 \text{ such that } d_p^{ap}(p_1, p_2) = c\}$$

are ellipses centered on p_1 with principal axes (p_{1x}, p_{1y}) and $(-p_{1y}, p_{1x})$ and lengths c and $c\sqrt{1 + \frac{\|p_1\|^2}{L^2}}$ (see Figure 2).

B. Distance point to segment

In this subsection we give an expression of the distance point to segment (1). Let us consider a point p_1 and a line segment defined by two points s_1 and s_2. The distance between p_1 and segment $[s_1\ s_2]$ is defined by:

$$d_{ps}(p_1, [s_1\ s_2]) = \min_{\lambda \in [0,1]} d_p(p_1, (1-\lambda)s_1 + \lambda s_2) \quad (7)$$

Let us denote by $d(\lambda) = d_p(p_1, (1-\lambda)s_1 + \lambda s_2)$ the distance between p_1 and the point on segment $[s_1\ s_2]$ of parameter λ. Following the same reasoning as in previous Section, we can approximate this distance by:

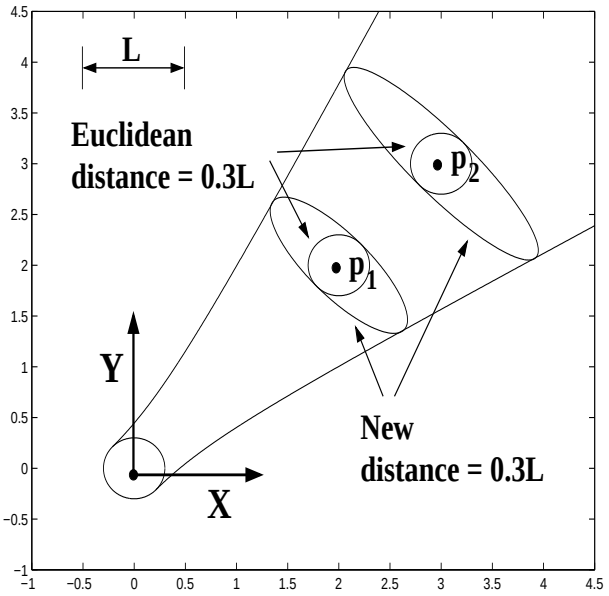

Fig. 2. The iso-distance curves of d_p^{ap} are ellipses centered on p_1.

$$d(\lambda)^2 \approx \delta_x(\lambda)^2 + \delta_y(\lambda)^2 - \frac{(\delta_x(\lambda) p_{1y} - \delta_y(\lambda) p_{1x})^2}{p_{1y}^2 + p_{1x}^2 + L^2} \quad (8)$$

where

$$\delta(\lambda) = (\delta_x(\lambda), \delta_y(\lambda)) = s_1 - p_1 + \lambda(s_2 - s_1) \quad (9)$$

Substituting (9) into (8), we get a polynomial of degree 2 in λ:

$$d(\lambda)^2 \approx a\lambda^2 + b\lambda + c$$

with the following coefficients:

$$\begin{aligned} a &= u_{2x}^2 + u_{2y}^2 - \frac{(p_{1y} u_{2x} - p_{1x} u_{2y})^2}{p_{1x}^2 + p_{1y}^2 + L^2} \\ b &= 2(u_{2x}\delta_{1x} + u_{2y}\delta_{1y}) \\ &\quad -2\frac{(p_{1y} u_{2x} - p_{1x} u_{2y})(\delta_{1x} p_{1y} - \delta_{1y} p_{1x})}{p_{1x}^2 + p_{1y}^2 + L^2} \\ c &= \delta_{1x}^2 + \delta_{1y}^2 - \frac{(\delta_{1x} p_{1y} - \delta_{1y} p_{1x})^2}{p_{1x}^2 + p_{1y}^2 + L^2} \end{aligned}$$

where $u_2 = (u_{2x}, u_{2y}) = s_2 - s_1$ and $\delta_1 = (\delta_{1x}, \delta_{1y}) = s_1 - p_1$. Coefficient a is positive and therefore the above expression has a unique minimum in λ, for $\lambda = \frac{-b}{2a}$ with value $\frac{-b^2+4ac}{4a}$. The expression of the approximation of the distance $d_{ps}(p_1, [s_1\ s_2])$ for small rotations is thus given by:

$$d_{ps}(p_1, [s_1\ s_2]) \approx \begin{cases} d_p(p_1, s_1) & \text{if } \lambda < 0 \\ d_p(p_1, s_2) & \text{if } \lambda > 1 \\ \sqrt{\frac{-b^2+4ac}{4a}} & \text{if } 0 \le \lambda \le 1 \end{cases}$$

and the closest point to p_1 on $[s_1\ s_2]$ in these three cases is respectively s_1, s_2 and $s_1 - \frac{b}{2a}s_2$.

C. Least Square Minimization

To compute the q that minimizes the criterion proposed in (2), we use the following notation: the coordinates of p_i (reference points) and p_i'' (new points in reference system, $q_k(p_i')$) are respectively (p_{ix}, p_{iy}) and (p_{ix}'', p_{iy}''). Using the approximate distance (6), we get the following expression:

$$E_{dist}(q) = \sum_{i=1}^{n} \left(\delta_{ix}^2 + \delta_{iy}^2 - \frac{(\delta_{ix} p_{iy} - \delta_{iy} p_{ix})^2}{p_{iy}^2 + p_{ix}^2 + L^2} \right) \quad (10)$$

where

$$\begin{aligned} \delta_{ix} &= p_{ix}'' - p_{iy}''\theta + x - p_{ix} \\ \delta_{iy} &= p_{ix}''\theta + p_{iy}'' + y - p_{iy} \end{aligned}$$

(10) is quadratic w.r.t. q:

$$E_{dist}(q) = q^T A q - 2 b^T q + c$$

where c is a constant number, A is a symmetric matrix

$$A = \begin{pmatrix} a_{11} & a_{12} & a_{13} \\ a_{12} & a_{22} & a_{23} \\ a_{13} & a_{23} & a_{33} \end{pmatrix}$$

$a_{11} = \sum_{i=1}^{n} p_{ix}^2 + L^2$
$a_{12} = \sum_{i=1}^{n} p_{ix} p_{iy}$
$a_{13} = \sum_{i=1}^{n} p_{ix}'' p_{ix} p_{iy} - p_{iy}''(p_{ix}^2 + L^2)$
$a_{22} = \sum_{i=1}^{n} p_{iy}^2 + L^2$
$a_{23} = \sum_{i=1}^{n} -p_{iy}'' p_{ix} p_{iy} + p_{ix}''(p_{iy}^2 + L^2)$
$a_{33} = \sum_{i=1}^{n} p_{ix}''(p_{iy}^2 + L^2) + p_{iy}''(p_{ix}^2 + L^2) - 2 p_{ix}'' p_{iy}'' p_{ix} p_{iy}$

and

$$b = \begin{pmatrix} \sum_{i=1}^{n} (p_{ix}'' - p_{ix})(p_{ix}^2 + L^2) + (p_{iy}'' - p_{iy}) p_{ix} p_{iy} \\ \sum_{i=1}^{n} (p_{ix}'' - p_{ix}) p_{ix} p_{iy} + (p_{iy}'' - p_{iy})(p_{iy}^2 + L^2) \\ \sum_{i=1}^{n} (p_{ix}'' - p_{ix})[p_{ix}'' p_{ix} p_{iy} - p_{iy}''(p_{ix}^2 + L^2)] \\ +(p_{iy}'' - p_{iy})[-p_{iy}'' p_{ix} p_{iy} + p_{ix}''(p_{iy}^2 + L^2)] \end{pmatrix}$$

The value of q that minimizes $E_{dist}(q)$ is thus

$$q_{min} = A^{-1} b$$

IV. Experimental Results

In this Section we outline the experimental results. We tested the method with data obtained with a wheelchair mobile robot equipped with a Sick laser scanner.

In order to compare our method (metric-based ICP, MbICP in short) with existing scan matching techniques, we used the standard ICP and the widely known IDC algorithm [14]. The IDC algorithm uses two types of correspondences (translation and rotation) and interpolates in both between successive range points (local structure). This method is designed to deal with large rotation errors. We did not implement this last method *ad hoc* for the comparison, since we have this tool working in our laboratory [17], [15], [16]. In our implementation, we reject outliners using visibility criteria [14] and range criterions [18]. Furthermore we use a trimmed version of the ICP to manage the correspondences [5] that improves the least squares minimization, and a smooth criterion of convergence [18]. We also implemented these features in the ICP and the MbICP algorithm. In order to show a fair comparison, we used the same values for common parameters (actually we used our IDC previous parameters for the ICP and MbICP), and we only tuned the metric length in the MbICP (the only *ad hoc* parameter). In the experiments, we found that $L = 3$ gave the best results.

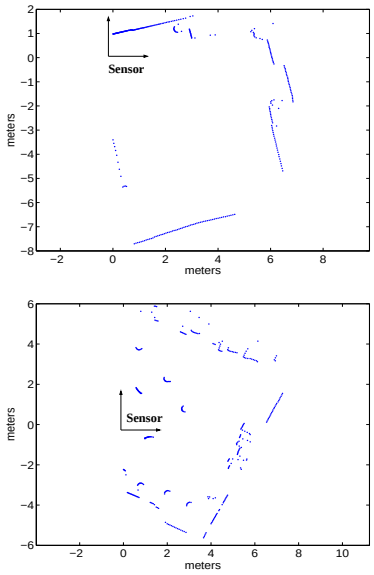

Fig. 3. Scans used in the experiment: one in a semi-structured with low density of obstacles and another in an unstructured with high density.

We outline next two types of experiments. The first evaluates the properties of the MbICP algorithm by matching a pair of scans for random location errors. The second one evaluates the global algorithm performance with a run with the vehicle within our university (Figures 5 and 6).

The first experiment consisted on matching two different scans acquired in the same sensor location. Thus, the scans are different due to the sensor noise and we know precisely the ground truth $(0, 0, 0)$. We added random noise to the initial location estimate up to 0.2m in x and y, and up to $45°$ in θ. Notice how large are the maximum errors especially in rotation [1]. Convergence of the algorithm was achieved when the error ratio was below 0.0001% and the maximum number of iterations was 500. We perform this test in two different scenarios (Figure 3). The scans were taken in a place where the range information was more or less equally distributed in all directions, which is a well-conditioned situation for the methods. We repeated each experiment 500 times for each scenario (a total of 1000 runs).

Figure 4a depicts the final estimates of the MbICP, IDC and ICP. The MbICP and IDC converged all the times and all the estimates concentrate around the true solution $(0, 0, 0)$. In other words, all the results of the MbICP and IDC were *True Positive* (see Table below). On the other hand, in 1.1% of the trials the ICP did not converge leading to negatives. Another measure of robustness is that some of the ICP positives were *False Positives*. They corresponded to situations were the ICP converged but

[1] Previous comparisons of scan matching [18] use maximum rotation errors up to $6°$.

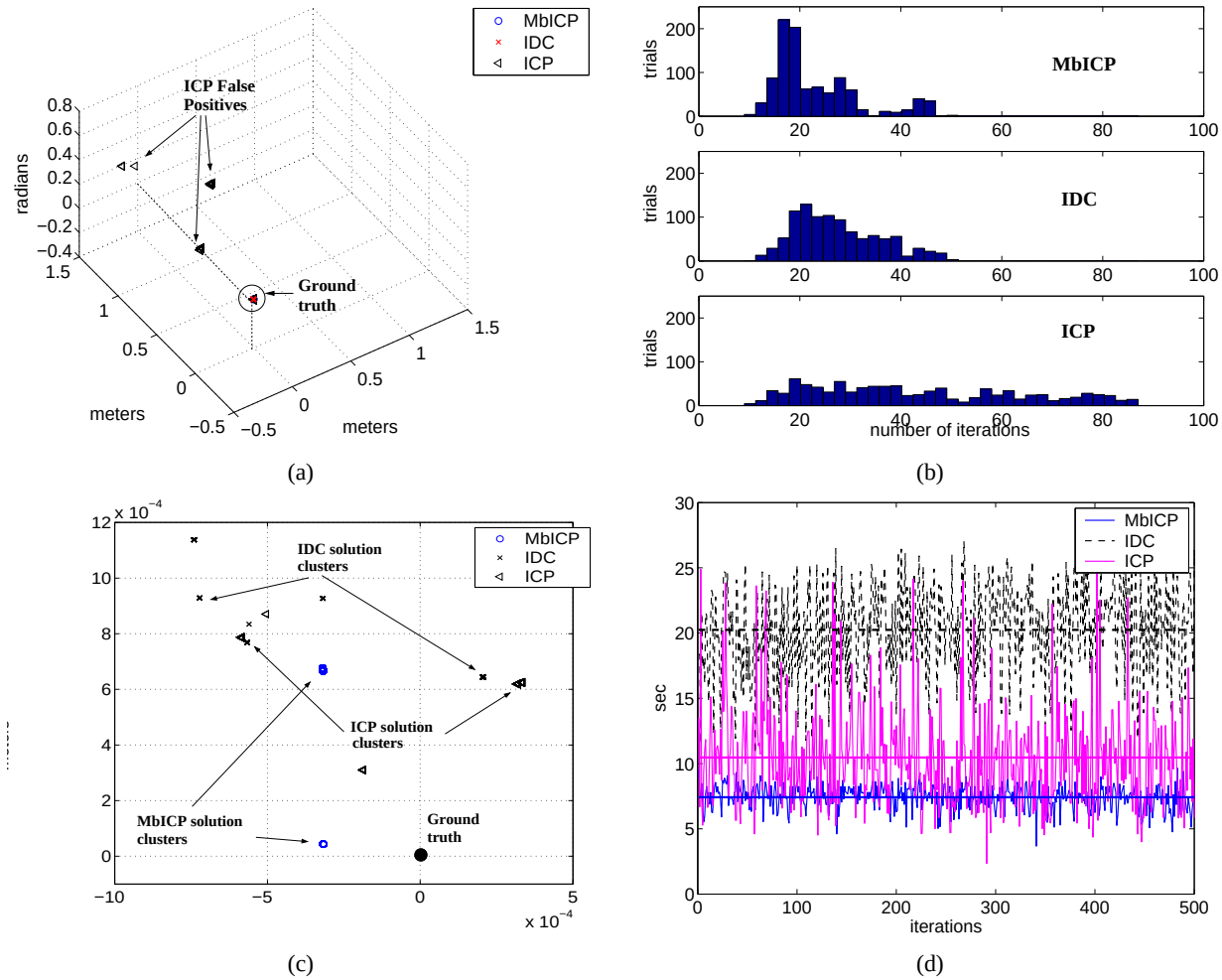

Fig. 4. (a) Estimations of both algorithms. (b) Convergence rate (without the ICP negatives). (c) Zoom on the estimations around the ground truth projected in the XY plane. (d) Computation time (without the ICP negatives), where the horizontal line is the mean time.

towards a local minimum that did not correspond to the real solution (Figure 4a).

TABLE I
MBICP VS IDC AND ICP (%)

	Positive	False Positive	Negative	False Negative
MbICP	100	0	0	0
IDC	100	0	0	0
ICP	92.9	6	1.1	0

These results show that the MbICP and the IDC are more robust than the ICP: (i) all the results of the MbICP and IDC were *True Positives* while the ICP had *Negatives* (they correspond to large errors in orientation that could not be compensated). And (ii) the ICP had 1.1% of *False Positives* (also due to large errors in orientation) which are really bad for these methods since the estimate is wrong although the result is positive. The MbICP is as robust as the IDC facing large errors in rotation (our method performs as good as methods designed to deal with these situations).

Figure 4c depicts a zoom on Figure 4a projected on the XY plane. All the solutions of the MbICP concentrate closer to the ground truth than the solutions of the IDC and ICP. They tend to concentrate in two different clusters for each scan and algorithm. Next table depicts the mean and standard deviation of the error in both coordinates (we only use the *True positives*):

TABLE II
MBICP VS IDC AND ICP ERROR

	x error		y error		th error	
	μ	σ	μ	σ	μ	σ
MbICP (10^{-3})	0.3	0.001	0.4	0.31	0.0	0.0
IDC (10^{-3})	0.4	0.22	0.8	0.16	0.0	0.0
ICP (10^{-3})	0.3	0.13	0.4	0.16	0.0	0.0

When the algorithm converges to the right solution, the medium and covariance of the errors are very similar. The MbICP seems more accurate than IDC, but the errors are so small (sub millimetre precision) that are not significant.

Figure 4b depicts the number of iterations for each trial. The converge rate is better in the MbICP than in the IDC and ICP. Figure 4d shows the computation time of the algorithms [2]. The MbICP takes half time than the IDC. This is because the IDC performs two sets of associations

[2]Although the times displayed were obtained off-line using Matlab, our C implementation of the IDC (on the vehicle) runs at a medium of 0.020sec (the ratio is about $\frac{1}{1000}$).

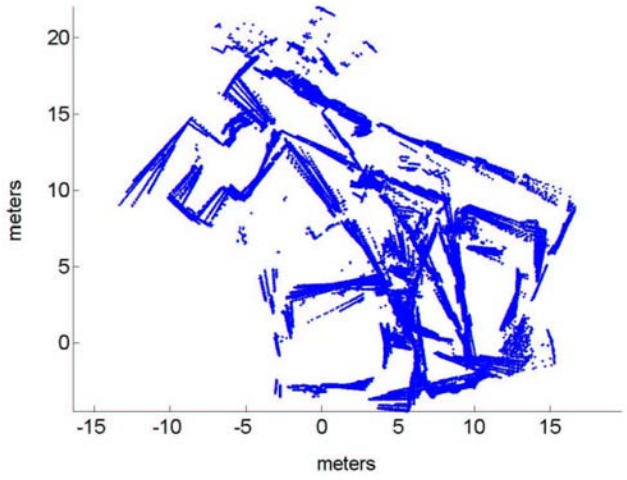

Fig. 5. This Figure depicts the odometry data of a trial of 70 meters.

and two minimizations while the MbICP and ICP only one. Also, the MbICP is faster than the ICP since it always converges before.

We remark that this test was carried out with large errors in translation and rotation. This experiment illustrates how the MbICP is as robust and precise as methods designed to have good performance under these conditions, and it is better than the standard ICP. Furthermore, the MbICP converges more rapid and is faster than previous methods. Although we have tried to give the maximum generality with the scans selected, the conclusions given are valid for these scans. To confirm these results we present next an experiment with real motion in a real scenario.

The second experiment corresponds to a run in our University with the wheelchair vehicle. The robot travelled 70 meters getting out of an office, travelling around a corridor and coming back to the office. The experiment is difficult because the floor was very polished and the vehicle slipped constantly with a poor effect on the odometry (Figure 5). In addition, the scenario was full of chairs, tables, baskets which are non structured, and the corridor is quite long and thus there was not many frontal structure to correct the location in this direction.

Figure 6 depicts the results obtained with the MbICP and the IDC. We see how the visual result of the MbICP is better than the IDC since it is able to align the corridor and the office when it comes back. The rotational accumulated error is lower for the MbICP than for the IDC. Moreover, note how the error in translation is also quite small. In this experiment the scans changed from one iteration to another (involving issues as spurious and new parts of the scenario). The mean convergence rate was 27 iterations for the MbICP and 33 for the IDC. Thus, these experiments show how under more realistic conditions the behavior of the MbICP is globally better than in the IDC (robustness, accuracy and convergence).

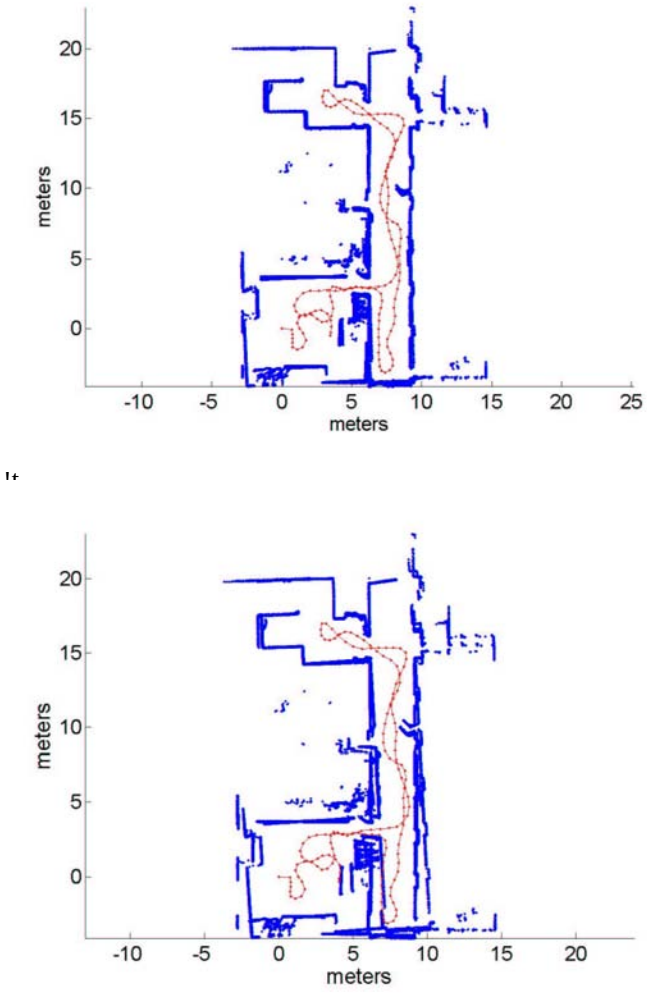

Fig. 6. (Top) Visual map obtained with the MbICP. (Bottom) Visual map of the IDC.

V. Conclusions

This paper presents a metric-based matching algorithm to estimate the robot planar displacement by matching dense two-dimensional range scans. The contribution is a geometric distance that takes into account the translation and orientation of the sensor at the same time.

We have implemented and tested the technique in a real vehicle and compared with the widely used Iterative Dual Corresponce scan matching (IDC) algorithm and the standard ICP. The results demonstrate that we improve previous methods in robustness, precision, convergence rate and computation time. This is because we compensate at the same time the three variables of the minimization (two of translation and one of rotation). Another important consequence is that our method is able to deal with large odometry errors especially in rotation, which is the difficulty of most of the existing approaches and has deserved a lot of discussion in this discipline.

Finally we address in the next Section how this technique could be extended to be used in other contexts.

VI. Discussion and Future Work

In this Section we describe extensions of this metric based scan matching technique. The first issue to address is how to extend the metric to deal with more complex systems (with crossrelations in the coordinates). This could be done by extending the norm to be:

$$||q||^2 = q^T A q \tag{11}$$

where $A = \{a_{i,j}, i, j = 1 \dots 3\}$ is a symmetric and semipositive matrix. The expression of the distance is then:

$$d^{ap} = |\delta^T Q \delta|^{\frac{1}{2}} \tag{12}$$

where $\delta = (\delta_x \ \delta_y)^T$ and:

$$Q = \begin{pmatrix} a_{11} - \frac{k_2^2}{2k_1} & a_{12} - \frac{k_2 k_3}{4k_1} \\ a_{12} - \frac{k_2 k_3}{4k_1} & a_{22} - \frac{k_3^2}{2k_1} \end{pmatrix} \tag{13}$$

$$\begin{aligned} k_1 &= a_{11}p_y^2 + a_{22}p_x^2 - 2a_{12}p_x p_y - \\ &\quad - 2a_{23}p_x + 2a_{33}p_y + a_{33} \\ k_2 &= 2(a_{11}p_y - a_{12}p_x + a_{33}) \\ k_3 &= 2(a_{12}p_y - a_{22}p_x + a_{23}) \end{aligned}$$

This expression of the distance is the generalization of the distance presented in this paper. This would allow to address the same problem but describing more complex systems.

Another important matter is the extension of the distance formulation to three dimensions. Up to now we have demonstrated that the distance is also a distance in $\mathbf{R}^3$ and the expression given two points p_1 and p_2 is:

$$d^{ap} = ||p_2 - p_1||^2 - \frac{||p_1 \otimes p_2||^2}{||p_1||^2 + L^2} \tag{14}$$

This result allows to address scan matching problems in 3D workspaces and to use it in other communities that use the ICP algorithm to address sensor motion estimation, location and map building, object recognition, pattern analysis, image registration, and scene understanding among others. Up to our knowledge the idea of a unified framework to take into account translation and rotation in the ICP has not been explored in these communities yet [19].

Finally, we are exploring how this distance relates with an statistical distance called the Mahalanobis distance. More precisely, by associating the matrix A with the information matrix of vector q, and transforming it to the point location using the Jacobian of q, we obtain a matrix C defining the uncertainty of the point location. The Mahalanobis distance using C is equal to the expression of our approximate distance. However, we remark that this is true for the approximate expression of the distance (obtained linearizing). In any case, we stress that, to our knowledge, the scan- matching problem has not been addressed with the Mahalanobis distance yet. The results of this paper suggest promising research opportunities in this direction.

VII. Acknowledgments

This work was partially supported by MCYT DPI2003-7986, DGA2004T04 and the *Caja de Ahorros de la Inmaculada de Aragón*.

References

[1] O. Bengtsson and A.-J. Baerveldt. Localization by matching of range scans - certain or uncertain? In *EURobot'01*, Lund, Sweden, 2001.

[2] P. Besl and N. McKay. A method for registration of 3-d shapes. *IEEE Transactions on Pattern Analysis and Machine Intelligence*, 14:239–256, 1992.

[3] P. Biber and W. Strafler. The normal distributions transform: A new approach to laser scan matching. In *IEEE Int. Conf. on Intelligent Robots and Systems*, Las Vegas, USA, 2003.

[4] J. A. Castellanos, J. D. Tardós, and J. Neira. Constraint-based mobile robot localization. In *Advanced Robotics and Intelligent Systems*, IEE, Control Series 51, 1996.

[5] D. Cheverikov, D. Svirko, and P. Krsek. The trimmed iterative closest point algorithm. In *International Conference on Pattern Recognition*, volume 3, pages 545–548, 2002.

[6] I. Cox. Blanche: An experiment in guidance and navigation of an autonomous robot vehicle. *IEEE Transactions on Robotics and Automation*, 7:193–204, 1991.

[7] J. Gonzalez and R. Gutierrez. Direct motion estimation from a range scan sequence. *Journal of Robotics Systems*, 16(2):73–80, 1999.

[8] A. Grossmann and R. Poli. Robust mobile robot localization from sparse and noisy proximetry readings using hough transform and probability grids. *Robotics and Autonomous Systems*, 37:1–18, 2001.

[9] J.-S. Gutmann and K. Konolige. Incremental mapping of large cyclic environments. In *Conference on Intelligent Robots and Applications (CIRA)*, Monterey, CA, 1999.

[10] J.-S. Gutmann and C. Schlegel. Amos: Comparison of scan matching approaches for self-localization in indoor environments. In *1st Euromicro Workshop on Advanced Mobile Robots*, 1996.

[11] D. Hähnel, D. Fox, W. Burgard, and S. Thrun. A highly efficient fastslam algorithm for generating cyclic maps of large-scale environments from raw laser range measurements. In *IEEE/RSJ International Conference on Intelligent Robots and Systems*, Las Vegas, Usa, 2003.

[12] S. Lacroix, A. Mallet, D. Bonnafous, G. Bauzil, S. Fleury, M. Herrb, and R. Chatila. Autonomous rover navigation on unknown terrains: Functions and integration. *International Journal of Robotics Research*, 21(10-11):917–942, Oct-Nov. 2002.

[13] Y. Liu. Improving icp with easy implementation for free form surface matching. *Pattern Recognition*, 37:211–226, 2004.

[14] F. Lu and E. Milios. Robot pose estimation in unknown environments by matching 2d range scans. *Intelligent and Robotic Systems*, 18:249–275, 1997.

[15] J. Minguez, L. Montesano, and L. Montano. An architecture for sensor-based navigation in realistic dynamic and troublesome scenarios. In *IEEE Int. Conf. on Intelligent Robot and Systems*, Sendai, Japan, 2004.

[16] L. Montesano, J. Minguez, and L. Montano. Modeling the static and the dynamic parts of the environment to improve sensor-based navigation. In *IEEE International Conference on Robotics and Automation (ICRA)*, 2005.

[17] L. Montesano and L. Montano. Identification of moving objects by a team of robots using kinematic information. In *IEEE Int. Conf. on Intelligent Robots and Systems (IROS)*, pages 284–290, 2003.

[18] S. Pfister, K. Kreichbaum, S. Roumeliotis, and J. Burdick. Weighted range sensor matching algorithms for mobile robot displacement estimation. In *In Proceedings of the IEEE International Conference on Robotics and Automation (ICRA)*, pages 1667–74, 2002.

[19] S. Rusinkiewicz and M. Levoy. Efficient variants of the icp algorithm. In *International Conference 3DIM*, 2001.

[20] D. Schulz, W. Burgard, D. Fox, and A. Cremers. Tracking Multiple Moving Targets with a Mobile Robot using Particle Filters and Statistical Data Association. In *IEEE Int. Conf. on Robotics and Automation*, Seoul, Korea, 2001.

[21] C.-C. Wang, C. Thorpe, and S. Thrun. Online simultaneous localization and mapping with detection and tracking of moving objects: Theory and results from a ground vehicle in crowded urban areas. In *Proceedings of the IEEE International Conference on Robotics and Automation (ICRA)*, 2003.

[22] G. Weiss and E. von Puttkamer. A map based on laserscans without geometric interpretation. In *Intelligent Autonomous Systems 4 (IAS-4)*, 1995.